 doi:10.1111/j.1365-2958.2011.07523.x

# A bacterial dynamin-like protein mediating nucleotide-independent membrane fusion

**Frank Bürmann,[†] Nina Ebert, Suey van Baarle[‡] and Marc Bramkamp***
*Institute for Biochemistry, University of Cologne, Zülpicherstr. 47, 50674 Köln, Germany.*

## Summary

**Dynamins are a family of large GTPases that are involved in key cellular processes, where they mediate events of membrane fission and fusion. The dynamin superfamily is not restricted to eukaryotes but might have a bacterial origin, with many species containing an operon of two genes related to mitofusins. However, it is not clear whether bacterial dynamins promote membrane fission or fusion. The dynamin-like protein DynA of *Bacillus subtilis* is remarkable in that it arose from a gene fusion of two dynamins and contains two separate dynamin-like subunits and GTPase domains. We found that DynA exhibits strictly auto-regulated GTP hydrolysis, and that progress through the GTPase cycle is concerted within DynA oligomers. Furthermore, we show that DynA can tether membranes and mediates nucleotide-independent membrane fusion *in vitro*. This process merely requires magnesium as a cofactor. Our results provide a set of minimal requirements for membrane fusion by dynamin-like proteins and have mechanistic implications in particular for the fusion of mitochondria.**

## Introduction

GTPases of the dynamin superfamily are involved in a variety of cellular processes and are major mediators of membrane remodelling in eukaryotes (Praefcke and McMahon, 2004). Mammalian dynamin 1 is the founding member of its protein family and is involved in the detachment of endocytic vesicles from the plasma membrane (van der Bliek and Meyerowitz, 1991; Herskovits *et al*., 1993; van der Bliek *et al*., 1993). It is able to form large helical assemblies around the necks of budding vesicles (Hinshaw and Schmid, 1995; Takei *et al*., 1995), shows assembly stimulated GTPase activity (Warnock *et al*., 1996) and promotes vesicle fission by a nucleotide dependent conformational change. This might comprise constriction (Sweitzer and Hinshaw, 1998), longitudinal expansion (Stowell *et al*., 1999) or rotation (Roux *et al*., 2006) of the helix. Furthermore, bilayer destabilization by membrane binding and release cycles has been proposed (Bashkirov *et al*., 2008; Pucadyil and Schmid, 2008).

Dynamin GTPases also conduct central steps of mitochondrial membrane dynamics (Hoppins *et al*., 2007). Key mediators of these processes are Dnm1/DRP1, Mgm1/OPA1 and the fuzzy onions (Fzo1)/mitofusins, all of which are members of the dynamin superfamily. These components are conserved among eukaryotes, and mutations in some of the human homologues are cause of severe neurodegenerative disease (Knott *et al*., 2008). Dnm1/DRP1 is the single dynamin responsible for the fission of mitochondria, and is located at the cytoplasmic site of the outer mitochondrial membrane (Bleazard *et al*., 1999). Mitochondrial fusion on the other hand requires two distinct complexes of dynamins, with Fzo1/mitofusins acting on the outer membrane and Mgm1/OPA1 performing the fusion of inner membranes. Mitofusins are anchored to the mitochondrial surface via transmembrane helices (Hoppins *et al*., 2007) and interactions between mitofusin complexes on adjacent membranes are regulated by nucleotide (Ishihara *et al*., 2004; Koshiba *et al*., 2004). However, the mechanism of how membrane fusion is achieved following the tethering process is unknown. After outer membrane fusion is completed, inner membranes are tethered by Mgm1/OPA1, ultimately leading to their fusion (Meeusen *et al*., 2006).

Since the dynamin superfamily has diverse functions in eukaryotes, it is not surprising that it has emerged early in evolution (van der Bliek, 1999; Leipe *et al*., 2002). Indeed, many bacterial species contain genes encoding dynamin-like proteins, which are most closely related to the Fzo1/mitofusins class (van der Bliek, 1999; Leipe *et al*., 2002; Low and Löwe, 2006). However, a function of bacterial

Accepted 17 December, 2010. *For correspondence. E-mail marc.bramkamp@uni-koeln.de; Tel. (+49) 221 4706472; Fax (+49) 221 4705091. Present addresses: [†]Max Planck Institute of Biochemistry, Am Klopferspitz 18, 82152 Martinsried, Germany; [‡]Biological Sciences Building, Department of Biological Sciences, University of Alberta, Edmonton, AB, Canada.

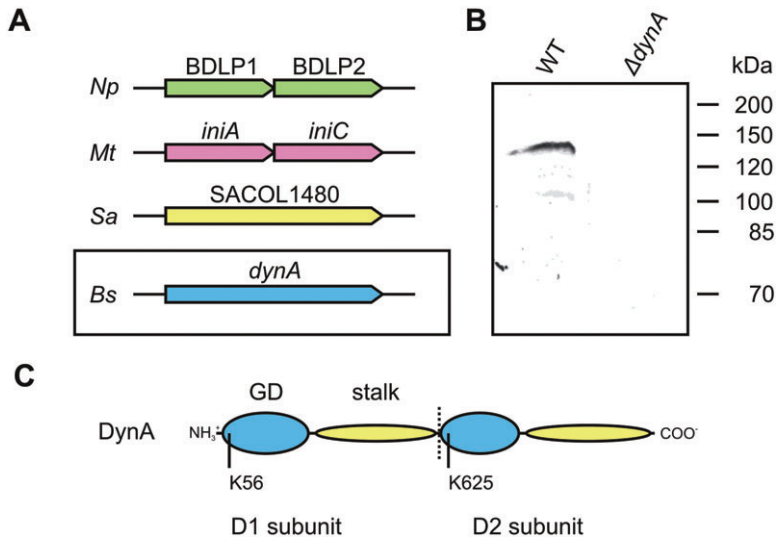


**Fig. 1.** DynA is a fusion protein of two bacterial dynamins.
A. Genomic organization of bacterial dynamins. *Np*, *Nostoc punctiforme*; *Mt*, *Mycobacterium tuberculosis*; *Sa*, *Staphylococcus aureus* COL; *Bs*, *Bacillus subtilis*.
B. Western blot analysis with α-DynA$_{D2}$ antibodies. DynA is present in the membrane fraction of wild-type *B. subtilis* as a full-length protein and absent in the deletion strain Δ*dynA*.
C. Schematic representation of the DynA molecule. The protein contains two GTPase domains (GD) and helical regions probably corresponding to the stalk region (trunk, neck and paddle domains) of BDLP1 (Low and Löwe, 2006). Positions of the P-loop lysines K56 and K625 are indicated.

dynamins remains unknown. Nevertheless, detailed structural data exist. The structure of bacterial dynamin-like protein 1 (BDLP1) from *Nostoc punctiforme* has been solved in both its nucleotide-free and GDP-bound states (Low and Löwe, 2006), revealing a similar architecture to the distantly related human guanylate binding protein 1 (hGBP1) (Prakash *et al*., 2000). BDLP1 is able to assemble on the surface of liposomes as a helical polymer, deforming its membrane template into highly curved tubules and perturbing the outer lipid layer (Low *et al*., 2009). The polymer itself is stabilized by contacts between GTPase and stalk domains, respectively, reminiscent of interactions found in other dynamin family members (Chappie *et al*., 2010; Gao *et al*., 2010; Pawlowski, 2010).

Interestingly, many bacterial species – including *N. punctiforme* – contain more than one dynamin gene, with two of them often found in tandem (Fig. 1A, Fig. S1 and Table S1). The organization in an operon probably indicates close functional relationship, with some species even harbouring a fusion of the two dynamin genes containing two GTPase domains. One of the two-headed bacterial dynamins is the protein encoded by the *ypbR* locus of *Bacillus subtilis* which we term DynA (Fig. 1C). The roles of eukaryotic dynamin-like proteins in membrane remodelling processes led us to speculate whether the bacterial dynamin-like proteins might also be involved in membrane fusion or fission. Fusion of membranes in *B. subtilis* takes place during the late stages of cytokinesis and at completion of prespore engulfment during sporulation. Here, we focused on a biochemical analysis of the *B. subtilis* DynA protein and its enzymatic characteristics and show that it is capable of tethering and merging membranes *in vitro*.

## Results and discussion

### *DynA is a dynamin-like GTPase*

In *B. subtilis*, DynA is present in the membrane as a 137 kDa full-length protein and is not processed into separate dynamin subunits (Fig. 1B), suggesting that the components of bacterial two-dynamin systems might generally act in close proximity. Sequence analysis of DynA suggests that it does not harbour transmembrane segments, but rather might bind to membranes as described for the *N. punctiforme* BDLP1 protein (Low and Löwe, 2006). The GTP-binding domains of DynA show similarity to GTPase domains from other dynamin-like proteins such as BDLP1 and eukaryotic members of the dynamin protein family (Fig. S1 and Table S1).

To investigate its molecular properties, we expressed DynA in *Escherichia coli* and purified it by chromatography (Fig. S2). The protein was nucleotide-free as determined by HPLC (Fig. 2A). A central motif in the GTPase domain is the P-loop, which contains an essential lysine residue that contributes to nucleotide binding (Fig. S1 and Saraste *et al*., 1990). We analysed GTP-binding to recombinant DynA and its P-loop mutants using UV-cross-linking of [α-$^{32}$P]-GTP (Fig. 2B). Single P-loop mutants (K65A and K625A) still bind GTP, whereas GTP-binding is fully abolished when both P-loops are mutated. Purified DynA displays GTPase activity and is inactivated by introduction of mutations into both P-loops (Fig. 2C). Interestingly, GTPase activity of the single P-loop mutants DynA$_{K56A}$ and DynA$_{K625A}$ is also abolished (Fig. 2D). It therefore seems likely that both GTPase domains of a given DynA molecule are required to bind nucleotide in order to complete the hydrolysis cycle. This model is in agreement with the finding that GTP hydrolysis of wild-type protein is cooperative with respect to

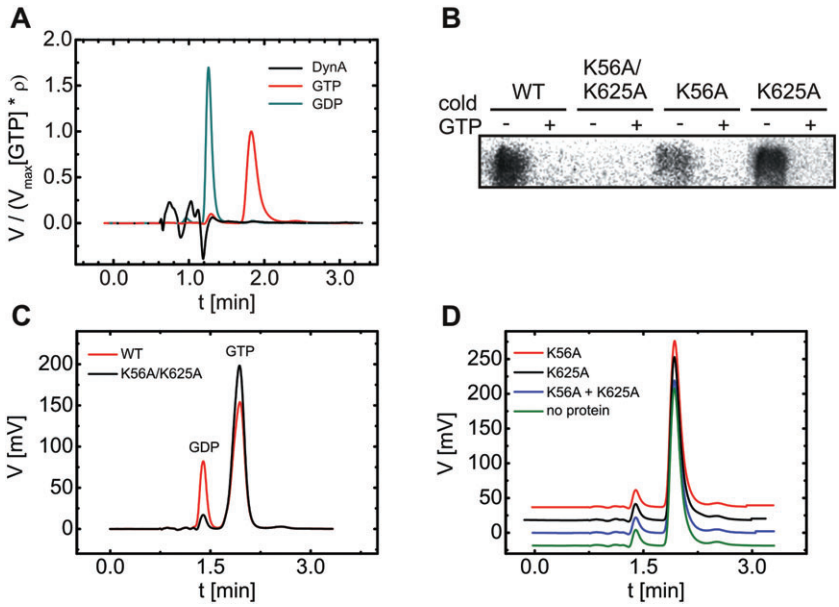


**Fig. 2.** DynAK56A and DynAK625A do not hydrolyse GTP.
A. Purified DynA is nucleotide free. Equal volumes of 25 μM protein,1 mM GTP or GDP were analysed by HPLC and voltage was normalized to the GTP peak scaled by the ratio ρ between analyte concentration and GTP concentration (ρ = c[analyte]/c[GTP]).
B. GTP binding to DynA was assayed by UV-cross-linking to [α-$^{32}$P]-GTP. Binding was quenched with 1 mM cold GTP where indicated.
C. One-micromolar protein (DynA, red curve and K56A/K625A, black curve) were incubated for 10 min at 25°C in the presence of 1 mM GTP and 5 mM $MgSO_4$ and reaction products were analysed by HPLC.
D. Single P-loop mutants and a mixture of K56A and K625A are catalytically inactive.

substrate concentration with a $K_{0.5}$ of 0.12 ± 0.02 mM, a $V_{max}$ of 3.9 ± 0.14 min$^{-1}$ and a Hill constant of 2.3 ± 0.6 at 0.25 μM protein (Fig. 3A). The kinetic data suggest that hydrolysis by a given GTPase domain is sensitive to the nucleotide bound state of another GTPase domain. Because activity is not reconstituted when both single P-loop mutants are mixed (Fig. 2D), cooperativity is likely exhibited between GTPase domains of the same polypeptide and cannot be provided *in trans*. Consistently, truncated versions of the protein lacking either the N-terminal or C-terminal GTPase subunit are also unable to perform hydrolysis (data not shown).

In addition, we noticed a weak activation of the protein in the presence of liposomes (Fig. 3A). Since the specific

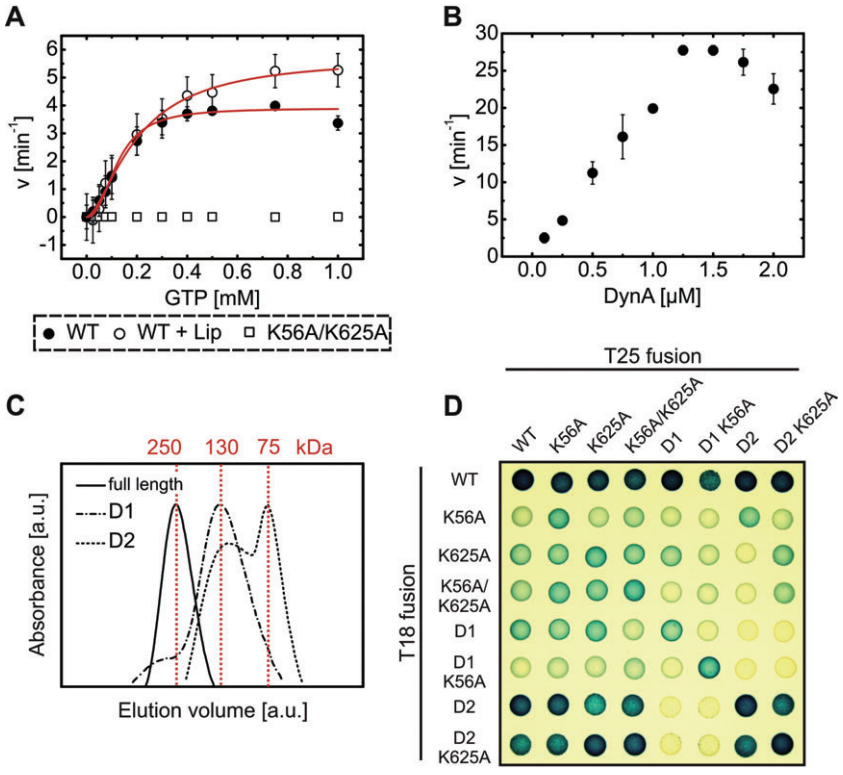


**Fig. 3.** DynA is a self-interacting GTPase.
A. GTPase activity of 0.25 μM DynA in the presence and absence of 0.2 mg ml$^{-1}$ liposomes compared with the double P-loop mutant K56A/K625A.
B. Specific activity at 1 mM GTP over a range of DynA concentrations. Error bars indicate the standard error of three independent experiments.
C. Size exclusion analysis of full-length DynA and its N-terminal ($DynA_{D1}$) and C-terminal ($DynA_{D2}$) subunits in the absence of nucleotide.
D. Two-hybrid interaction matrix of DynA and its subunits with respect to P-loop mutations.

activity of DynA is sensitive to protein concentration (Fig. 3B), we believe that this effect might be due to accumulation of DynA on the membrane surface. In summary, DynA displays two modes of cooperativity: First, there is intramolecular cooperativity between the two GTPase domains of a given DynA molecule, and second there is intermolecular cooperativity in which DynA stimulates GTP hydrolysis of partner molecules.

### *GTPase subunits of DynA show self-interaction symmetry*

As predicted by the kinetic analysis, we indeed observed self-interaction of the protein. DynA forms dimers in the nucleotide-free state as determined by size exclusion chromatography (Fig. 3C). Truncated versions of DynA, lacking either the C-terminal dynamin subunit ($DynA_{D1}$, 71.2 kDa) or the N-terminal subunit ($DynA_{D2}$, 74.4 kDa), are also able to oligomerize, with $DynA_{D2}$ forming dimers and $DynA_{D1}$ forming dimers and probably tetramers (Fig. 3C). Therefore, both subunits of DynA can provide homotypic contacts for complex formation.

To test whether self-interaction might be influenced by GTPase activity, we constructed fusions of P-loop mutants to *Bordetella pertussis* adenylate cyclase T18 and T25 fragments and performed two-hybrid analysis in *E. coli* (Fig. 3D). The assay reported interaction signals for full-length proteins and also displays homotypic interactions for truncated D1 and D2 subunits, which is consistent with the observations obtained by gel filtration. Since the nucleotide binding and hydrolysis assays indicate that GTPase defective mutants of DynA are trapped in different stages of nucleotide loading, they may therefore provide a crude stop motion picture through this process. In the two-hybrid assay, P-loop mutants gave most intense signals when self-interaction was tested (visible on the diagonal from upper left to lower right in the matrix and also reported by interactions of the truncated versions), indicating that the probability of complex formation is highest when both proteins are in a symmetrical GTP bound state. Put differently, stability of the complex might be low when the molecules are *not* in the same state. Since heterotypic interactions between T18 and T25 constructs compete with homotypic interactions between T18 or T25 tagged molecules that do not reconstitute adenylate cyclase activity, the two-hybrid assay is sensitive to relative expression levels. T18 constructs were expressed from a high-copy vector, whereas T25 fusions were expressed from a low-copy plasmid. Wild-type DynA generally gave strong signals when it was expressed from the high-copy vector and tested against constructs expressed from the low-copy vector. Signals were drastically reduced when the expression ratio was reversed. We believe that this reflects the ability of wild-type DynA to complete its hydrolysis cycle and to enter all nucleotide bound states, enabling it to efficiently form complexes with each of the mutant proteins when it is in excess. The generally increased signal intensity of the T18 wild-type construct might be explained by a low stability of the hydrolytically active complex. This would minimize unproductive interactions between T18-tagged constructs and shift the equilibrium towards the formation of more stable, hydrolytically inactive complexes with adenylate cyclase activity. It should be noted, however, that signals reported by the two-hybrid assay might also partially reflect conformational changes other than changes in oligomerization.

### *DynA is able to tether membranes via its D1 subunit*

In contrast to *N. punctiforme* BDLP1 which shows nucleotide modulated membrane affinity (Low *et al.*, 2009), DynA displayed nucleotide-independent membrane binding *in vitro* (Fig. 4A). Also in live *B. subtilis*, GFP-tagged DynA stayed associated with the cell periphery when nucleotide binding was disrupted (Fig. 4C). Since we additionally introduced a *dynA* deletion it can be excluded that mutant DynA–GFP is recruited to the membrane by wild-type protein. To investigate the contributions of the N- and C-terminal subunits to membrane binding, we expressed GFP fusions of $DynA_{D1}$ or $DynA_{D2}$. Only $DynA_{D1}$–GFP was found to be membrane associated, whereas $DynA_{D2}$–GFP displayed cytoplasmic localization (Fig. 4C). This membrane binding behaviour was also observed for purified components. DynA and $DynA_{D1}$ co-sedimented with liposomes, whereas $DynA_{D2}$ did not (Fig. 4B). It should be noted, however, that although $DynA_{D1}$ was clearly shifted to the pellet fraction in the presence of liposomes, it also partially sedimented in the absence of liposomes. The purified construct is therefore more likely reflecting membrane binding in a rather qualitative than quantitative way. Binding to the membrane surface was confirmed by electron microscopy, which showed ordered self-assembly of DynA in the absence of nucleotide (Fig. 5).

Strikingly, full-length DynA was not only able to bind to liposomes, but also tethered them into large clusters as was readily observed by light microscopy and turbidimetry (Fig. 6B and C). The D1 subunit was required and sufficient for this effect (Fig. 6C). In addition to this, we also observed the formation of extensive tethering zones between adjacent cellular compartments when DynA–GFP was expressed in yeast (Fig. 6A). Since D1 seems to be the membrane binding subunit and was sufficient for tethering, the DynA oligomer is likely in a conformation, which is able to cross-link opposing membranes via separate D1 subunits.

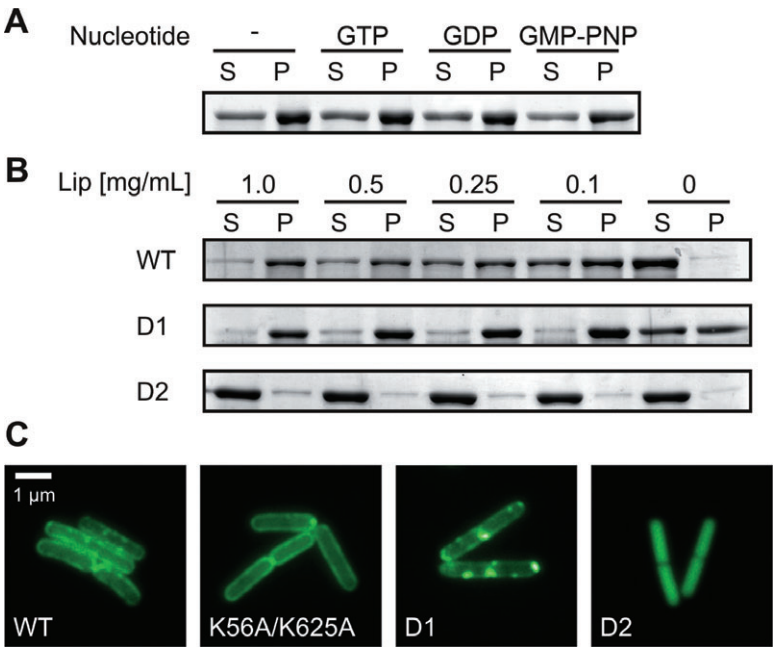


**Fig. 4.** Nucleotide-independent membrane binding of DynA via its N-terminal dynamin subunit.
A. Liposome sedimentation of DynA in the presence of different nucleotides (1 mM). Shown are Coomassie stained protein bands.
B. Liposome sedimentation assay with purified proteins in the absence of nucleotides (S, supernatant; P, pellet).
C. Localization of GFP-labelled constructs in a Δ*dynA* background.

*DynA promotes nucleotide-independent membrane fusion*

Because DynA was able to act as an efficient bilayer tether, we asked if it was also able to promote membrane fusion. We performed lipid mixing assays with 4-nitrobenzo-2-oxa-1,3-diazole (NBD) and rhodamine head-group-labelled lipids (Struck *et al*., 1981). These fluorophors form a Förster resonance energy transfer (FRET) pair, which is diluted into the membrane of unla-

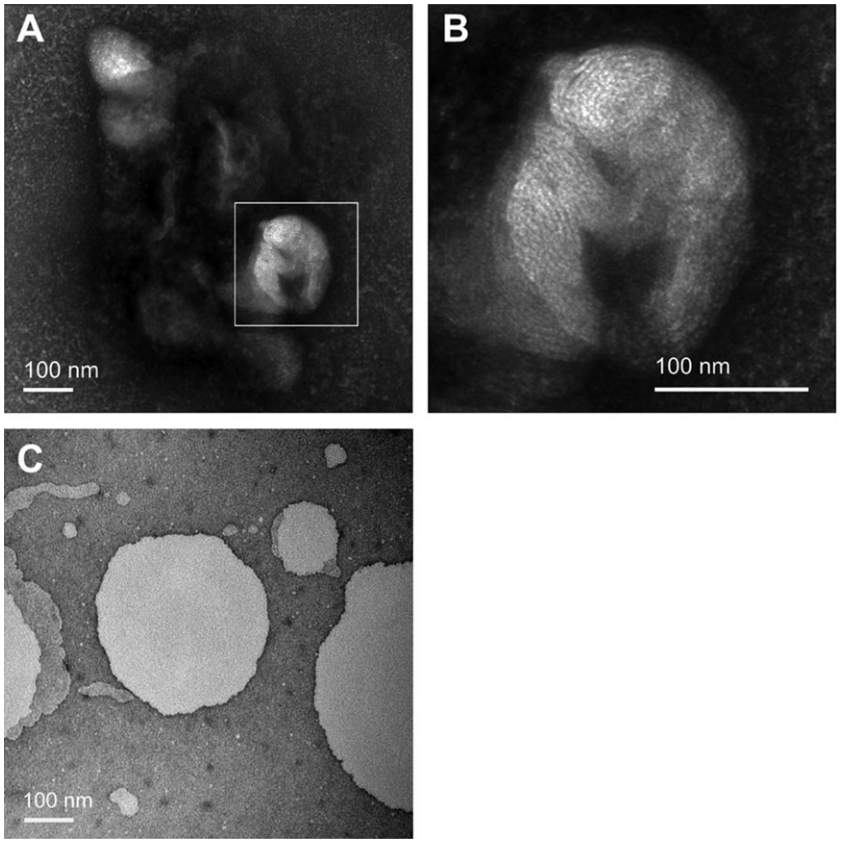


**Fig. 5.** DynA exhibits ordered self-assembly on liposomes.
A. Liposomes incubated with 25 µM DynA in the absence of nucleotide were examined by electron microscopy.
B. Magnification of ordered structures formed by DynA on the surface of the liposomes.
C. Liposomes without protein.

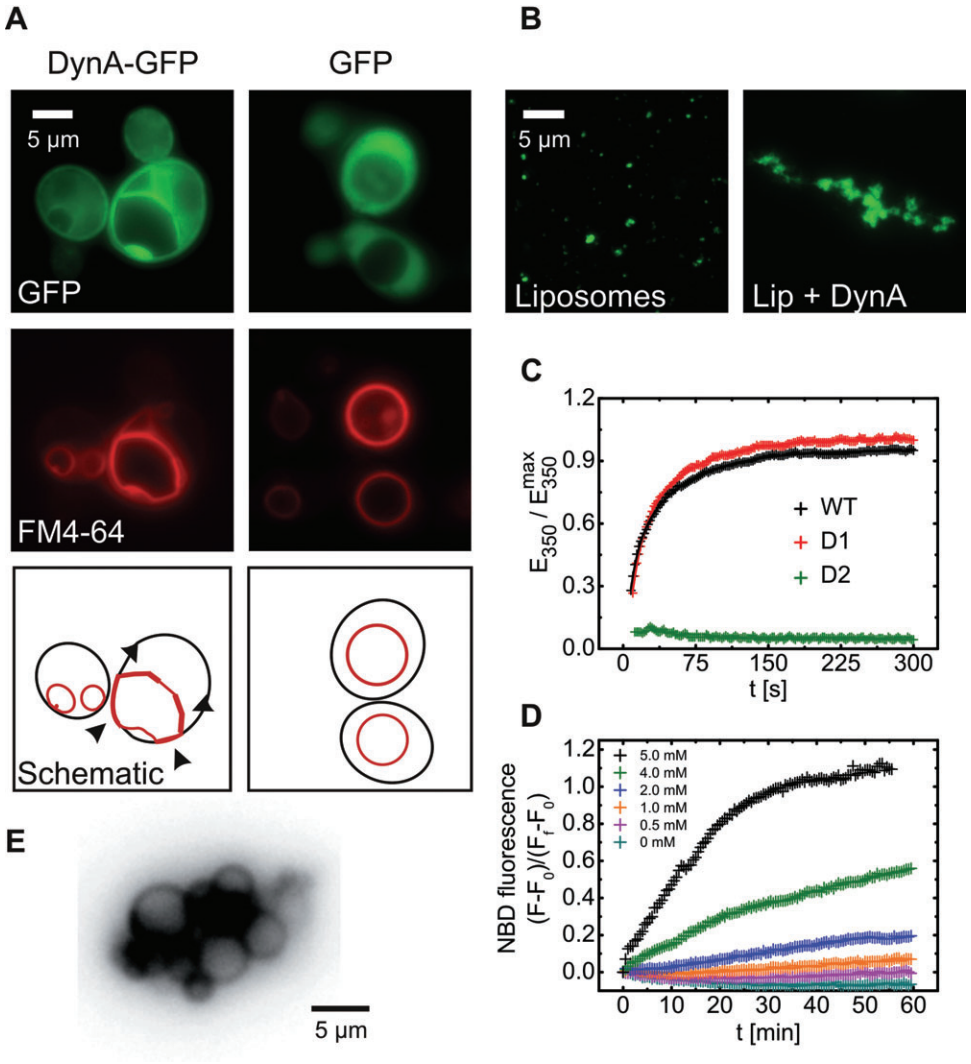


**Fig. 6.** DynA is able to tether and fuse membranes.
A. Introduction of DynA–GFP (left) into *Saccharomyces cerevisiae* but not GFP alone (right) leads to the formation of membrane tethering zones (arrowheads in cartoon). Vacuoles were stained with FM4-64.
B. Tethering of 0.2 mg $ml^{-1}$ NBD-PE labelled *E. coli* lipid liposomes in the presence of 2 µM DynA.
C. Aggregation of liposomes in the presence of 0.2 µM protein as measured by turbidity change at 350 nm.
D. FRET-based lipid mixing assay using NBD-PE/Rh-PE labelled donor liposomes and non-fluorescent acceptor liposomes in the presence of 0.2 µM DynA and the indicated $MgSO_4$ concentrations.
E. Nile red stained fusion products. Liposomes (400 nm) were fused and subsequently treated with proteinase K to remove the DynA coat.

belled acceptor liposomes upon membrane fusion. This results in impaired FRET efficiency, which can be monitored by changes in NBD fluorescence. Surprisingly, we observed extensive DynA-mediated liposome fusion in the absence of nucleotide but dependent on the presence of magnesium ions (Fig. 6D). Fusion did not take place in the presence of magnesium when protein was omitted from the reaction, but also occurred when DynA was substituted for $DynA_{K56A/K625A}$ or its D1 subunit (Fig. S3A). This shows that the fusion process is not driven by a nucleotide contamination of the lipid preparation, but is truly independent of nucleotide, and that the membrane binding and tethering subunit of DynA is sufficient for the process. In addition to this, we did not observe alterations in tethering or fusion behaviour when GTP was added to the reaction (Fig. S3B and C).

We noticed that liposome complexes did not undergo significant shape transitions during the fusion process, but stayed in the rather compact form also seen without magnesium. This shape might be generated by DynA coating. To visualize fusion products, we therefore treated fused liposome complexes with proteinase K to remove the DynA coat. Strikingly, under these conditions large vesicular fusion products could be observed (Fig. 6E),

showing that DynA catalyses complete fusion of both membrane leaflets.

Since free intracellular magnesium has been estimated to be in the low millimolar range in bacteria (Alatossava *et al*., 1985), the DynA fusion reaction may operate efficiently in a cellular environment. This is reminiscent of the magnesium-assisted membrane fusion of plant Golgi membranes, which has been shown to depend on an unidentified protein factor (Takeda and Kasamo, 2002). Indeed, magnesium ions are known to facilitate membrane fusion in areas of high membrane curvature and proximity (Wilschut *et al*., 1981). This effect might be explained by reduced charge repulsion between bilayers or an influence on lipid phase behaviour. Membrane proximity and potentially also curvature might be provided by DynA to overcome the kinetic barrier of membrane fusion. Another possibility we cannot yet exclude is that magnesium might bind to DynA directly and trigger the transition to a fusogenic conformation.

Our findings are likely relevant for fusion processes mediated by other dynamin-like proteins, like the fusion of mitochondrial membranes. For these processes, GTP hydrolysis might not be needed to energize fusion by means of mechanical force, but probably plays a regulatory role that determines if and how a dynamin complex tethers membranes and enters its fusogenic state. In their fusogenic state, dynamin-like proteins might then merely act as passive catalysts, promoting fusion simply by lowering the activation energy of bilayer merging. DynA might be an example for a dynamin-like protein that is – at least under the conditions used in this study – always in its active state.

### *DynA localizes to the sites of septation*

In *B. subtilis*, expression of DynA–GFP under control of the native promoter showed a preferred localization of DynA to the sites of septation (Fig. 7A and B). In order to corroborate the localization results we analysed the localization of DynA–GFP in absence of the division protein MinJ. We have chosen MinJ because it plays an important role in the mature divisome and makes protein–protein contacts to many membrane integral and membrane-associated division proteins (Bramkamp *et al*., 2008; van Baarle and Bramkamp, 2010). Strikingly, we observed a dramatic change in DynA localization in a Δ*minJ* strain background, showing a dispersed DynA localization along the entire cell membrane (Fig. 7C). Thus, DynA is very likely localized to the sites of septation making essential protein–protein contact with other cytokinetic proteins. These results might point to a role of bacterial dynamin-related proteins in cytokinesis, but since we did not observe a morphological phenotype for the Δ*dynA* strain, either surrogate systems might be expressed or bacterial dynamins might be important under specific environmental conditions. Of course at this stage we cannot entirely rule out that bacterial dynamins may be involved in other cellular functions.

## Conclusions

In addition to their homology to mitofusins, structural arguments (Low *et al*., 2009) and our experimental findings suggest that bacterial dynamins might be involved in a membrane fusion process, maybe taking place at the sites of septation. *In vitro* membrane fusion mediated by DynA, however, is in contrast to that performed by atlastins or mitofusins for which GTP hydrolysis is a prerequisite (Meeusen *et al*., 2004; Orso *et al*., 2009). This suggests that GTP hydrolysis is not generally needed to energize a dynamin-mediated fusion reaction and points to the existence of an ion-supported lipid mixing step. Our data suggest that dynamin-like proteins might not act as molecular machines but may act as regulated fusion catalysts. These molecules might have a fusogenic conformation, which can be switched on or off. Due to the evolutionary relationship between bacteria and mitochondria and the homology of bacterial dynamins to mitofusins, we think that these findings might be of particular relevance to the mechanism of mitochondrial fusion.

Although we did not observe a regulation of DynA-mediated fusion *in vitro*, we think that this might likely be the case *in vivo* due to the kinetic and self-interactive properties of the molecule. Since membrane binding and self-interaction are not operating uniformly in the dynamin superfamily, these properties are probably adapted to specific cellular roles. Fusion activity may depend on the membrane architecture and composition prevalent in the dynamin's cellular environment. Factors determining when, if and where a dynamin enters its fusogenic state might therefore define its function.

## Experimental procedures

### *Cloning and purification of DynA*

The *dynA* gene was cloned from *B. subtilis* 168 and inserted by NcoI and XhoI into pET16b (Novagen) with a C-terminal $His_6$ tag. Expression was performed overnight at 18°C with *E. coli* BL21(DE3) in Luria–Bertani (LB) with 0.5 mM IPTG and 50 μg $ml^{-1}$ carbenicillin. Cells were disrupted in 50 mM Tris, 200 mM NaCl, 20 mM imidazole, 10% glycerol, 1% Triton X-100, pH 8.0/4°C, and the protein was bound to Ni-NTA agarose (Qiagen). After extensive washing with 50 mM Tris, 500 mM NaCl, 20 mM imidazole, 10% glycerol, pH 8.0/4°C, protein was eluted in 50 mM Tris, 500 mM NaCl, 1 M imidazole, 10% glycerol, pH 8.0/4°C, reduced with 1 mM DTT and gel filtrated on Superdex 200 against 50 mM Tris, 500 mM

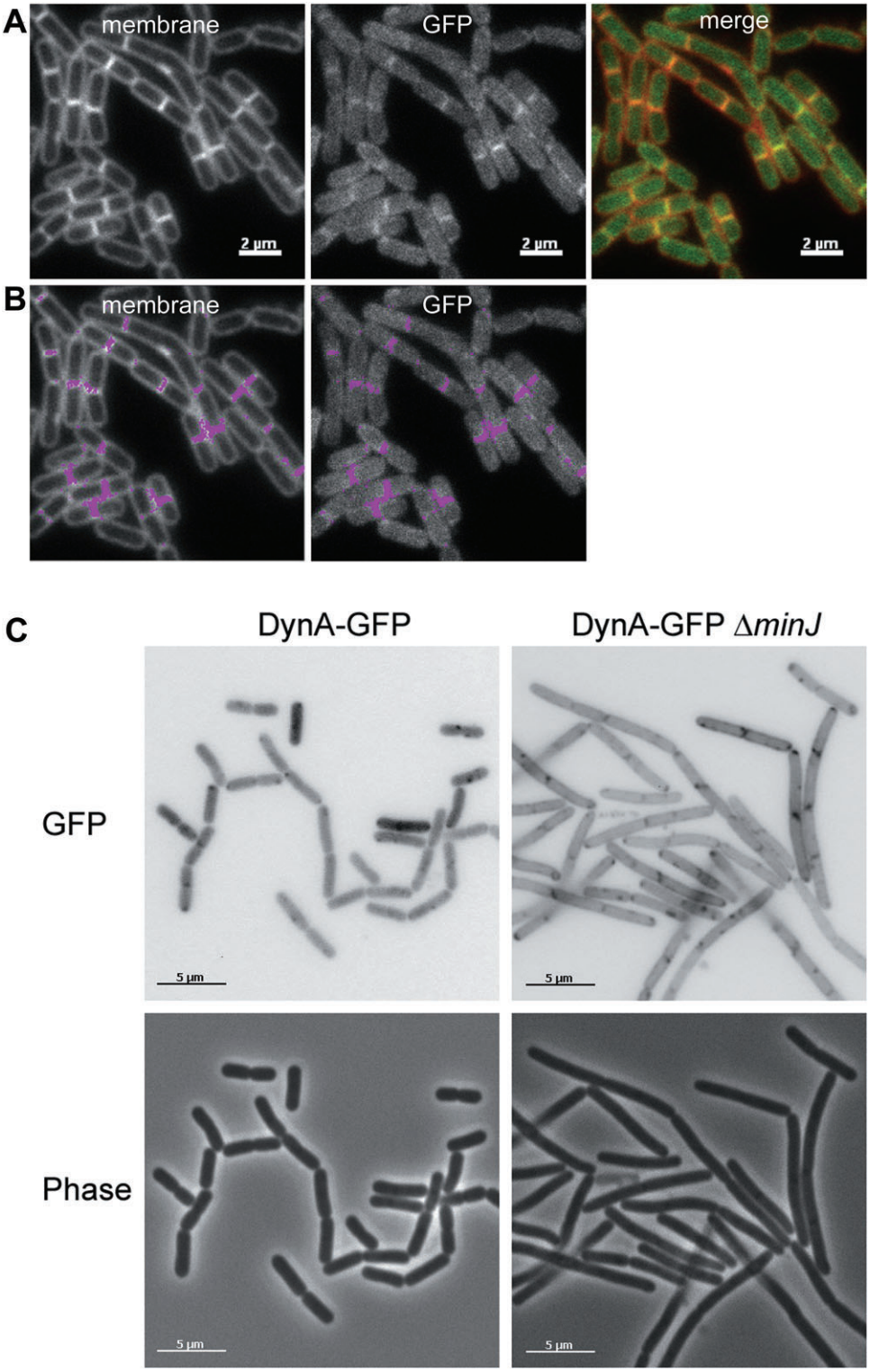


NaCl, 10% glycerol, pH 8.0/4°C. Purification of $DynA_{D1}$ (residues 1–609) and $DynA_{D2}$ (residues 561–1193) was analogous, except that lysis buffer of $DynA_{D1}$ contained 500 mM NaCl. All constructs contained an additional glycine in position 2 and a C-terminal GSS linker.

*Bacterial two-hybrid analysis*

For two-hybrid analysis, a system based on reconstitution of adenylate cyclase activity was used (Karimova *et al*., 2005). Sequences were cloned into pUT18C and pKT25 and trans-

**Fig. 7.** DynA localizes to the sites of septation.
A. *In vivo* localization of DynA–GFP expressed as single copy under its native promoter in *B. subtilis*. Shown are different channels as indicated. Membranes were stained with FM4-64.
B. Colocalization of DynA–GFP and membrane dye. The regions of colocalization are coloured in pink on top of the images showing the membrane and GFP channel images.
C. Altered DynA localization in absence of MinJ. Shown are cells in the logarithmic growth phase expressing DynA–GFP in otherwise wild-type background (left column) and in a Δ*minJ* background (right column). Note the redistribution of DynA–GFP all along the cell membrane in cells lacking MinJ.
The scale bars are 2 μm (A and B) and 5 μm in (C) respectively.

formed into *E. coli* BTH101. Cells were grown on LB with 160 mg ml$^{-1}$ X-Gal, 0.5 mM IPTG, 50 μg ml$^{-1}$ kanamycin and 100 μg ml$^{-1}$ carbenicillin at 30°C.

### *Generation of DynA–GFP strains and microscopy*

A list of strains can be found in Table S2. For genomic deletion of *dynA*, sequences approximately 250 bp up- and downstream of the gene were fused to a *tet* cassette via overlap extension PCR (Heckman and Pease, 2007). The construct was adenylated with *Taq* and cloned into pDRIVE (Qiagen). The targeting vector was linearized with ClaI and transformed into *B. subtilis*. For introduction of GFP-fusions into *B. subtilis*, sequences were cloned into pSG1154 via KpnI and XhoI and inserted into the *amyE* locus. Cells were induced in LB with 0% (DynA–GFP), 0.25% (DynA$_{D1}$–GFP) or 0.5% xylose (DynA$_{D2}$–GFP). The construct for expression of DynA–GFP under control of its native promoter was constructed by cloning the *dynA* gene including the promoter region into pSG1154. Expression from the pSG1154 intrinsic $P_{xyl}$ promoter was blocked by a transcriptional terminator upstream of $P_{dynA}$. A strain expressing DynA–GFP in absence of MinJ was constructed by transformation with chromosomal DNA of strain 3865 (Bramkamp *et al.*, 2008). Expression of GFP fusions in *S. cerevisiae* W303-1A(a) used the pYX223 vector and was performed in SC-His with 2% galactose. Vacuolar staining with FM4-64 was performed as described (Baars *et al.*, 2007). Microscopy was performed on a Zeiss AxioImager M1 equipped with an EC Plan-Neofluar 100x/1.3 Oil Ph3 objective and a Zeiss AxioCam HRm camera. Green fluorescence (GFP, NBD) was monitored using filter set 38 HE eGFP, and red fluorescence (FM4-64, Nile red) was monitored by using filter 43 HE Cy3.

### *GTPase activity measurement*

GTPase measurements were performed at 37°C in 50 mM Tris, 200 mM NaCl, 5 mM $MgSO_4$, 10% glycerol, pH 7.1/37°C by a coupled enzyme assay and corrected for spontaneous GTP hydrolysis (Ingerman *et al.*, 2005). Briefly, the indicated protein and GTP concentrations were incubated in the presence of 1 mM PEP, 0.6 mM NADH, 20 U ml$^{-1}$ pyruvate kinase and 20 U ml$^{-1}$ lactate dehydrogenase and a change in NADH concentration was monitored by absorbance at 340 nm.

### *UV-reactive cross-linking of [α-$^{32}$P]-GTP*

The GTP binding assay was performed as described before (Yue and Schimmel, 1977). Samples of 20 μl contained 3 μg protein, 1 μCi [α-$^{32}$P]-GTP in 50 mM Tris, 200 mM NaCl, 5 mM $MgSO_4$, 10% glycerol, pH 8.0/4°C. If required, 1 mM of unlabelled (cold) GTP was added. After incubation on ice for 10 min, UV irradiation was carried out at room temperature for 10 min at 0.1 J cm$^{-2}$ in a UV cross-linker (LTF Labortechnik). The samples were made up with 4 × SDS sample buffer and loaded onto an SDS-polyacrylamide gel (Tris/glycine 10% acrylamide gels were used throughout the study). Gels were stained for protein, dried under vacuum and exposed onto an imager plate (Raytest) for 2 days. The plate was scanned in a phosphorimager (Fujifilm BAS-1800) and images were processed using AIDA Image Analyzer software.

### *Liposome sedimentation assay*

*Escherichia coli* lipids (Avanti Polar Lipids) dissolved in chloroform were dried under nitrogen, exsiccated for 1 h and swollen at 37°C in 50 mM Tris, 10% glycerol, pH 7.1/37°C. The suspension was submitted to at least five freeze and thaw cycles, diluted to 2 mg ml$^{-1}$ in assay buffer and extruded through a 400 nm pore size filter. Then 2 μM protein was incubated for 20 min at 25°C with 1 mg ml$^{-1}$ liposomes in 50 mM Tris, 200 mM NaCl, 10% glycerol, pH 7.4/25°C, and the sample was fractionated by ultracentrifugation. Where indicated nucleotides were used at 1 mM with 5 mM $MgSO_4$.

### *Membrane preparation*

An overnight culture of *B. subtilis* was diluted 1:50 into LB and grown for 2 h at 37°C. Cells were harvested by centrifugation, resuspended in 50 mM Tris, 200 mM NaCl, 10% glycerol, pH 8.0/4°C and lysed in a tissue homogenizer. Cell debris was removed by centrifugation at 12 000 *g* for 10 min. Membranes were collected by centrifugation in a TLA 120.2 rotor at 80 000 r.p.m. for 20 min.

### *Liposome tethering and fusion assays*

Liposome tethering was observed at 20°C by sample turbidity changes at 350 nm with 0.2 μM protein and 0.2 mg ml$^{-1}$ liposomes in 50 mM Tris, 200 mM NaCl, 10% glycerol, pH 7.5/20°C. Liposome fusion was assayed at 37°C with 0.18 mg ml$^{-1}$ unlabelled acceptor liposomes and 0.02 mg ml$^{-1}$ donor liposomes labelled with 1.7% (w/w) NBD-PE and 2.4% (w/w) rhodamine-PE. NBD fluorescence was monitored with $\lambda_{ex} = 460$ nm and $\lambda_{em} = 538$ nm, and fluorescence change ($F - F_0$) was normalized to values after addition of 1% sodium dodecyl sulphate ($F_f - F_0$). For visualization of fusion products, unlabelled liposomes were fused in the presence of 2 μM DynA and 5 mM $MgSO_4$ and subsequently treated with

100 μg ml$^{-1}$ proteinase K. Products were stained with 10 μg ml$^{-1}$ Nile red immediately before imaging.

### *Electron microscopy*

The 0.2 mg ml$^{-1}$ preformed 400 nm liposomes made from *E. coli* total lipids (Avanti) were incubated with 25 μM DynA for 10 min at 37°C. Liposomes were subsequently negatively stained with uranyl acetate. The images were taken on a Philips CM100 Compustage Transmission Electron Microscope at the Newcastle EM Research Services.

### *Antibodies*

Antibodies against $DynA_{D2}$ were raised in rabbits and affinity purified with $DynA_{D2}$ coupled to CNBr sepharose. They were used at 1:3000 for Western blot analysis.

## Acknowledgements

We want to thank Gerrit Praefcke and Julia Fres (University of Cologne) for constructive criticism on the manuscript and for their help with HPLC measurements. We thank Reinhard Krämer (University of Cologne) for continuous support and the staff of the Newcastle Research Services (Newcastle University, UK) for help with electron microscopy.

## References

Alatossava, T., Jutte, H., Kuhn, A., and Kellenberger, E. (1985) Manipulation of intracellular magnesium content in polymyxin B nonapeptide-sensitized *Escherichia coli* by ionophore A23187. *J Bacteriol* **162:** 413–419.

Baars, T.L., Petri, S., Peters, C., and Mayer, A. (2007) Role of the V-ATPase in regulation of the vacuolar fission-fusion equilibrium. *Mol Biol Cell* **18:** 3873–3882.

Bashkirov, P.V., Akimov, S.A., Evseev, A.I., Schmid, S.L., Zimmerberg, J., and Frolov, V.A. (2008) GTPase cycle of dynamin is coupled to membrane squeeze and release, leading to spontaneous fission. *Cell* **135:** 1276–1286.

Bleazard, W., McCaffery, J.M., King, E.J., Bale, S., Mozdy, A., Tieu, Q., *et al.* (1999) The dynamin-related GTPase Dnm1 regulates mitochondrial fission in yeast. *Nat Cell Biol* **1:** 298–304.

van Baarle, S., and Bramkamp, M. (2010) The MinCDJ system in *Bacillus subtilis* prevents minicell formation by promoting divisome disassembly. *PLoS ONE* **5:** e9850.

van der Bliek, A.M. (1999) Functional diversity in the dynamin family. *Trends Cell Biol* **9:** 96–102.

van der Bliek, A.M., and Meyerowitz, E.M. (1991) Dynamin-like protein encoded by the *Drosophila shibire* gene associated with vesicular traffic. *Nature* **351:** 411–414.

van der Bliek, A.M., Redelmeier, T.E., Damke, H., Tisdale, E.J., Meyerowitz, E.M., and Schmid, S.L. (1993) Mutations in human dynamin block an intermediate stage in coated vesicle formation. *J Cell Biol* **122:** 553–563.

Bramkamp, M., Emmins, R., Weston, L., Donovan, C., Daniel, R.A., and Errington, J. (2008) A novel component of the division-site selection system of *Bacillus subtilis* and a new mode of action for the division inhibitor MinCD. *Mol Microbiol* **70:** 1556–1569.

Chappie, J.S., Acharya, S., Leonard, M., Schmid, S.L., and Dyda, F. (2010) G domain dimerization controls dynamin's assembly-stimulated GTPase activity. *Nature* **465:** 435–440.

Gao, S., von der Malsburg, A., Paeschke, S., Behlke, J., Haller, O., Kochs, G., and Daumke, O. (2010) Structural basis of oligomerization in the stalk region of dynamin-like MxA. *Nature* **465:** 502–506.

Heckman, K.L., and Pease, L.R. (2007) Gene splicing and mutagenesis by PCR-driven overlap extension. *Nat Protoc* **2:** 924–932.

Herskovits, J.S., Burgess, C.C., Obar, R.A., and Vallee, R.B. (1993) Effects of mutant rat dynamin on endocytosis. *J Cell Biol* **122:** 565–578.

Hinshaw, J.E., and Schmid, S.L. (1995) Dynamin self-assembles into rings suggesting a mechanism for coated vesicle budding. *Nature* **374:** 190–192.

Hoppins, S., Lackner, L., and Nunnari, J. (2007) The machines that divide and fuse mitochondria. *Annu Rev Biochem* **76:** 751–780.

Ingerman, E., Perkins, E.M., Marino, M., Mears, J.A., McCaffery, J.M., Hinshaw, J.E., and Nunnari, J. (2005) Dnm1 forms spirals that are structurally tailored to fit mitochondria. *J Cell Biol* **170:** 1021–1027.

Ishihara, N., Eura, Y., and Mihara, K. (2004) Mitofusin 1 and 2 play distinct roles in mitochondrial fusion reactions via GTPase activity. *J Cell Sci* **117:** 6535–6546.

Karimova, G., Dautin, N., and Ladant, D. (2005) Interaction network among *Escherichia coli* membrane proteins involved in cell division as revealed by bacterial two-hybrid analysis. *J Bacteriol* **187:** 2233–2243.

Knott, A.B., Perkins, G., Schwarzenbacher, R., and Bossy-Wetzel, E. (2008) Mitochondrial fragmentation in neurodegeneration. *Nat Rev Neurosci* **9:** 505–518.

Koshiba, T., Detmer, S.A., Kaiser, J.T., Chen, H., McCaffery, J.M., and Chan, D.C. (2004) Structural basis of mitochondrial tethering by mitofusin complexes. *Science* **305:** 858–862.

Leipe, D.D., Wolf, Y.I., Koonin, E.V., and Aravind, L. (2002) Classification and evolution of P-loop GTPases and related ATPases. *J Mol Biol* **317:** 41–72.

Low, H.H., and Löwe, J. (2006) A bacterial dynamin-like protein. *Nature* **444:** 766–769.

Low, H.H., Sachse, C., Amos, L.A., and Löwe, J. (2009) Structure of a bacterial dynamin-like protein lipid tube provides a mechanism for assembly and membrane curving. *Cell* **139:** 1342–1352.

Meeusen, S., McCaffery, J.M., and Nunnari, J. (2004) Mitochondrial fusion intermediates revealed *in vitro*. *Science* **305:** 1747–1752.

Meeusen, S., DeVay, R., Block, J., Cassidy-Stone, A., Wayson, S., McCaffery, J.M., and Nunnari, J. (2006) Mitochondrial inner-membrane fusion and crista maintenance requires the dynamin-related GTPase Mgm1. *Cell* **127:** 383–395.

Orso, G., Pendin, D., Liu, S., Tosetto, J., Moss, T.J., Faust, J.E., *et al.* (2009) Homotypic fusion of ER membranes requires the dynamin-like GTPase atlastin. *Nature* **460:** 978–983.

Pawlowski, N. (2010) Dynamin self-assembly and the vesicle scission mechanism: how dynamin oligomers cleave the membrane neck of clathrin-coated pits during endocytosis. *Bioessays* **32:** 1033–1039.

Praefcke, G.J., and McMahon, H.T. (2004) The dynamin superfamily: universal membrane tubulation and fission molecules? *Nat Rev Mol Cell Biol* **5:** 133–147.

Prakash, B., Renault, L., Praefcke, G.J., Herrmann, C., and Wittinghofer, A. (2000) Triphosphate structure of guanylate-binding protein 1 and implications for nucleotide binding and GTPase mechanism. *EMBO J* **19:** 4555–4564.

Pucadyil, T.J., and Schmid, S.L. (2008) Real-time visualization of dynamin-catalyzed membrane fission and vesicle release. *Cell* **135:** 1263–1275.

Roux, A., Uyhazi, K., Frost, A., and De Camilli, P. (2006) GTP-dependent twisting of dynamin implicates constriction and tension in membrane fission. *Nature* **441:** 528–531.

Saraste, M., Sibbald, P.R., and Wittinghofer, A. (1990) The P-loop – a common motif in ATP- and GTP-binding proteins. *Trends Biochem Sci* **15:** 430–434.

Stowell, M.H., Marks, B., Wigge, P., and McMahon, H.T. (1999) Nucleotide-dependent conformational changes in dynamin: evidence for a mechanochemical molecular spring. *Nat Cell Biol* **1:** 27–32.

Struck, D.K., Hoekstra, D., and Pagano, R.E. (1981) Use of resonance energy transfer to monitor membrane fusion. *Biochemistry* **20:** 4093–4099.

Sweitzer, S.M., and Hinshaw, J.E. (1998) Dynamin undergoes a GTP-dependent conformational change causing vesiculation. *Cell* **93:** 1021–1029.

Takeda, Y., and Kasamo, K. (2002) *In vitro* fusion of plant Golgi membranes can be influenced by divalent cations. *J Biol Chem* **277:** 47756–47764.

Takei, K., McPherson, P.S., Schmid, S.L., and De Camilli, P. (1995) Tubular membrane invaginations coated by dynamin rings are induced by GTP-γS in nerve terminals. *Nature* **374:** 186–190.

Warnock, D.E., Hinshaw, J.E., and Schmid, S.L. (1996) Dynamin self-assembly stimulates its GTPase activity. *J Biol Chem* **271:** 22310–22314.

Wilschut, J., Duzgunes, N., and Papahadjopoulos, D. (1981) Calcium/magnesium specificity in membrane fusion: kinetics of aggregation and fusion of phosphatidylserine vesicles and the role of bilayer curvature. *Biochemistry* **20:** 3126–3133.

Yue, V.T., and Schimmel, P.R. (1977) Direct and specific photochemical cross-linking of adenosine 5′-triphosphate to an aminoacyl-tRNA synthetase. *Biochemistry* **16:** 4678–4684.

## Supporting information

Additional supporting information may be found in the online version of this article.

Please note: Wiley-Blackwell are not responsible for the content or functionality of any supporting materials supplied by the authors. Any queries (other than missing material) should be directed to the corresponding author for the article.

## *SUPPLEMENTARY INFORMATION*

## *Supplementary figures*

**Supplementary figure 1| A**, Sequence alignment of bacterial and eukaryotic dynamin GTPase domains. Positions of the catalytic motives G1-G4 and the hhP motive characteristic for dynamin-like GTPases (Leipe et al., 2002) are highlighted. Accession codes and gene coordinates of the bacterial dynamins are listed in Table S1. It should be noted, however, that most *E. coli* strains seem to contain the *yjdA* gene as their sole dynamin. In the uropathogenic strain CFT073 the gene has probably been duplicated recently due to close homology between YjdA and the c2520 protein. **B**, Schematic representations of the bacterial dynamins used in (A). Positions of GTPase domains are indicated in green. *Bs, Bacillus subtilis*; *Np, Nostoc punctiforme*; *Sa, Staphylococcus aureus*; *Mt, Mycobacterium tuberculosis*; *Ec, Escherichia coli*; *Sc, Saccharomyces cerevisiae*; *Hs, Homo sapiens*.

**Table S1**:

| Protein | Origin | Accession code | Gene | Coordinates |
|---|---|---|---|---|
| DynA | *Bacillus subtilis* 168 | NP_390085 | *ypbR* | 2312529-2316110 |
| BDLP1 | *Nostoc punctiforme* ATCC 29133 | B2IZD3 | Npun_R6513 | 8049965-8052046 |
| BDLP2 | *Nostoc punctiforme* ATCC 29133 | B2IZD2 | Npun_R6512 | 8047218-8049440 |
| BDLP3 | *Nostoc punctiforme* ATCC 29133 | B2J872 | Npun_F0558 | 660034-662601 |
| BDLP4 | *Nostoc punctiforme* ATCC 29133 | B2IWD3 | Npun_R1152 | 1375040-1377487 |
| SACOL1480 | *Staphylococcus aureus* COL | Q5HFY2 | SACOL1480 | 1518288-1521728 |
| IniA | *Mycobacterium tuberculosis* CDC1551 | O06293 | MT0357 | 410898-412820 |
| IniC | *Mycobacterium tuberculosis* CDC1551 | O06294 | MT0357.1 | 412817-414298 |
| YjdA | *Escherichia coli* CFT073 | Q8FAU9 | c5114 | 4885671-4887899 |
| c2520 | *Escherichia coli* CFT073 | Q8FG72 | c2520 | 2358550-2360934 |

**Supplementary figure 2| Purification of DynA from *E. coli*. A**, Purification of full length DynA. **B**, Purification of $DynA_{D1}$. **C**, Purification of $DynA_{D2}$. L, lysate; F, flow through; Ni, protein after affinity chromatography; S, protein after size exclusion chromatography on Superdex 200.

**Supplementary figure 3| Tethering and fusion behaviour are not altered by GTP hydrolysis. A**, Lipid mixing measurement with $DynA_{K56A/K625A}$ and $DynA_{D1}$ in the presence or absence of 5 mM $MgSO_4$. **B**, Lipid turbidity measurement with 0.2 µM DynA in the presence or absence of 1 mM GTP and 5 mM $MgSO_4$. **C**, Lipid mixing in the presence of 1 mM GTP / 5 mM $MgSO_4$ and 0.2 µM DynA or 0.2 µM $DynA_{K56A/K625A}$.

Table S2. Bacterial and yeast strains[§]

| Strain | Relevant genotype/characteristic trait | Source |
|---|---|---|
| ***Bacillus subtilis*** | | |
| 168 | *trpC2* | Laboratory stock |
| 3865 | *yvjD::*pMUTIN4 *trpC2* | Bramkamp et al., 2008 |
| FBB002 | *dynA::tet trpC2* | This study |
| FBB018 | *amyE::Pxyl-dynA-gfp spc dynA::tet trpC2* | This study |
| FBB019 | *amyE::Pxyl-dynA[K56A, K625A]-gfp spc dynA::tet trpC2* | This study |
| NEB002 | *amyE::Pxyl-dynAD1-gfp spc dynA::tet trpC2* | This study |
| NEB003 | *amyE::Pxyl-dynAD2-gfp spc dynA::tet trpC2* | This study |
| NEB004 | *amyE::PdynA-dynA-gfp spc dynA::tet trpC2* | This study |
| NEB005 | *amyE::PdynA-dynA-gfp spc dynA::tet yvjD::*pMUTIN4*trpC2* | This study |

**Yeast**

| | | |
|---|---|---|
| *S. cerevisiae* W303-1A(a) | *MAT*a {*leu2-3,112 trp1-1 can1-100 ura3-1 ade2-1 his3-11,15*} | Laboratory stock |
| *S. cerevisiae* W303-1A(a)/ pYX223-GFP | *MAT*a {*leu2-3,112 trp1-1 can1-100 ura3-1 ade2-1 his3-11,15*} $GFP^+$ | This study |
| *S. cerevisiae* W303-1A(a)/ pYX223-DynA-GFP | *MAT*a {*leu2-3,112 trp1-1 can1-100 ura3-1 ade2-1 his3-11,15*} DynA-$GFP^+$ | This study |

***Escherichia coli***

| | | |
|---|---|---|
| BL21(DE3) | $F^-$ *ompT* [*lon*] *hsdS*$_B$ (*r*$_B^-$*m*$_B^-$) λ(DE3) *pol*(T7) | Novagen |
| BTH101 | $F^-$, *cya-99, araD139, galE15, galK16, rpsL1 (Str*$^r$*), hsdR2, mcrA1, mcrB1* | Euromedex |
| DH5α | $F^-$ *endA1 hsdR17 supE44 thi-a1* $\lambda^-$ *recA1 gyrA96 relA1* Δ(*lacZYA-argf*)U169 Φ80 Δ(*lacZ)M15* | Invitrogen |

§ Oligonucleotides and plasmids used in this study can be made available upon request.

**Figure S1**

**A**

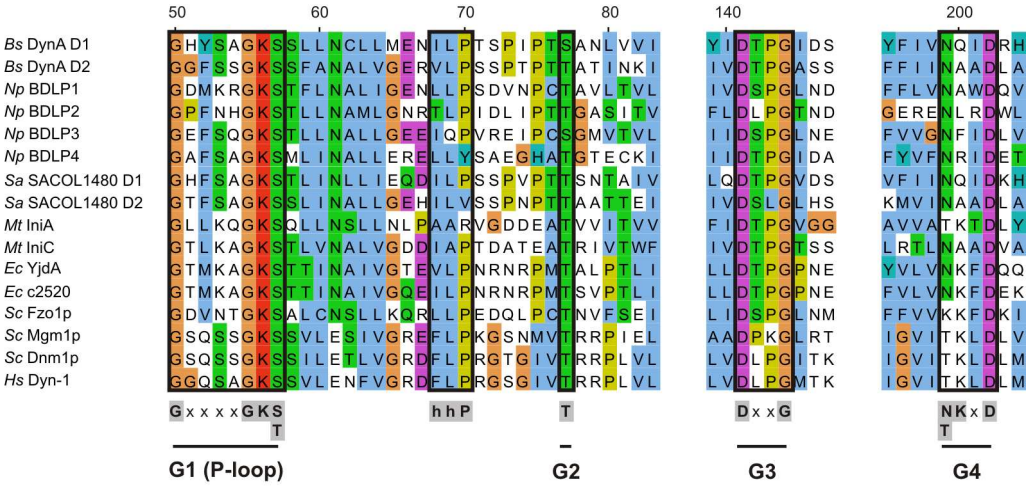
50
60
70
80
140
200
Bs DynA D1
Bs DynA D2
Np BDLP1
Np BDLP2
Np BDLP3
Np BDLP4
Sa SACOL1480 D1
Sa SACOL1480 D2
Mt IniA
Mt IniC
Ec YjdA
Ec c2520
Sc Fzo1p
Sc Mgm1p
Sc Dnm1p
Hs Dyn-1
G x x x x G K S T
h h P
T
D x x G
N K x D T
G1 (P-loop)
G2
G3
G4

**B**

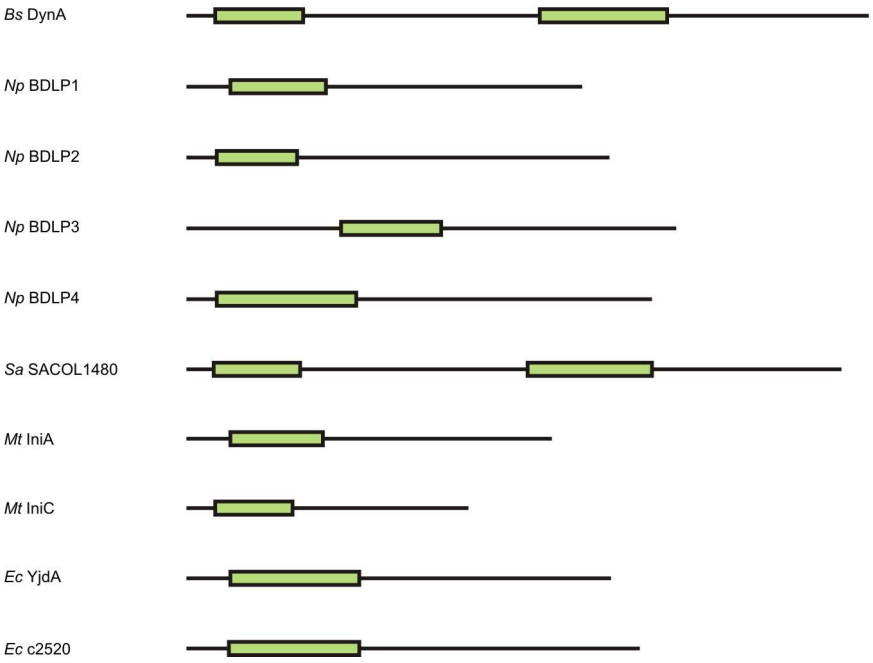
Bs DynA
Np BDLP1
Np BDLP2
Np BDLP3
Np BDLP4
Sa SACOL1480
Mt IniA
Mt IniC
Ec YjdA
Ec c2520

**Figure S2**

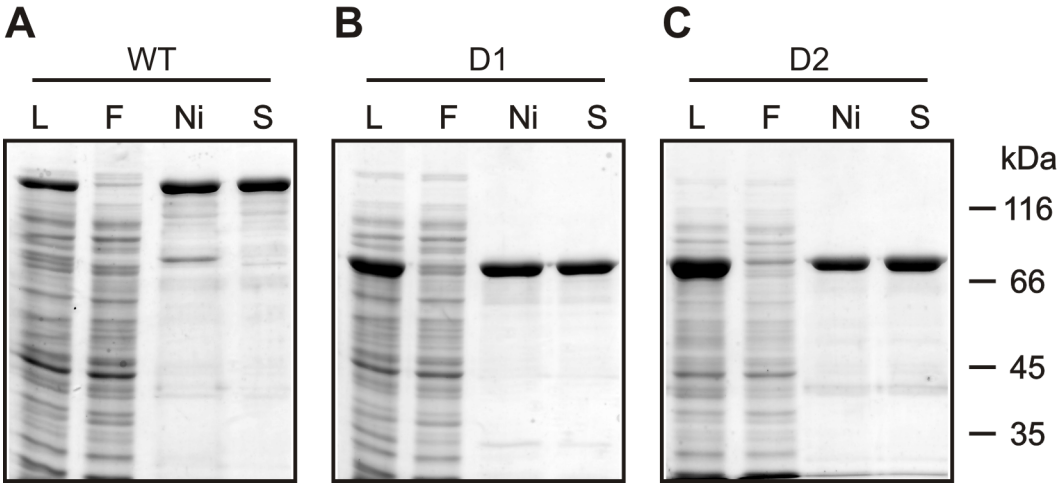

**Figure S3**

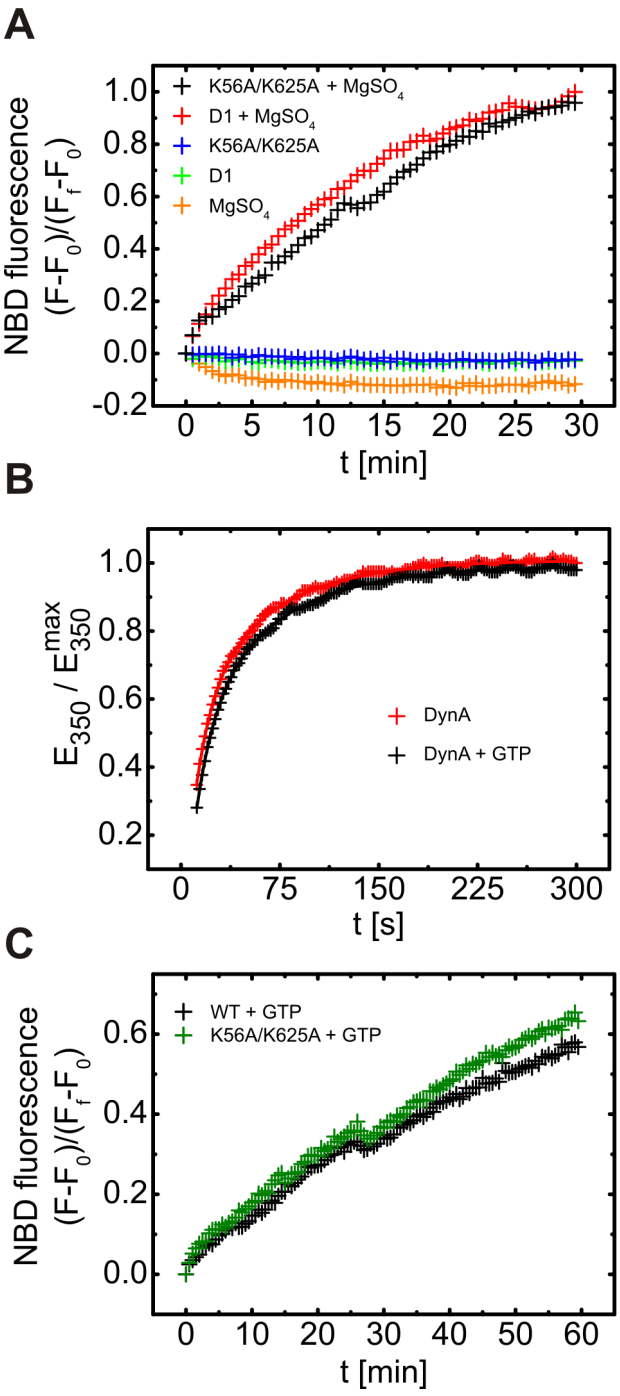
A
K56A/K625A + MgSO4
D1 + MgSO4
K56A/K625A
D1
MgSO4
NBD fluorescence
(F-F0)/(Ff-F0)
t [min]
B
DynA
DynA + GTP
E350 / E350max
t [s]
C
WT + GTP
K56A/K625A + GTP
NBD fluorescence
(F-F0)/(Ff-F0)
t [min]